

RDGCL: Reaction-Diffusion Graph Contrastive Learning for Recommendation

Jeongwhan Choi*
jeongwhan.choi@yonsei.ac.kr
Yonsei University
Seoul, South Korea

Hyowon Wi*
wihyowon@yonsei.ac.kr
Yonsei University
Seoul, South Korea

Chaejeong Lee
chaejeong_lee@yonsei.ac.kr
Yonsei University
Seoul, South Korea

Sung-Bae Cho
sbcho@yonsei.ac.kr
Yonsei University
Seoul, South Korea

Dongha Lee
donalee@yonsei.ac.kr
Yonsei University
Seoul, South Korea

Noseong Park[†]
noseong@yonsei.ac.kr
Yonsei University
Seoul, South Korea

ABSTRACT

Contrastive learning (CL) has emerged as a promising technique for improving recommender systems, addressing the challenge of data sparsity by leveraging self-supervised signals from raw data. Integration of CL with graph convolutional network (GCN)-based collaborative filterings (CFs) has been explored in recommender systems. However, current CL-based recommendation models heavily rely on low-pass filters and graph augmentations. In this paper, we propose a novel CL method for recommender systems called the reaction-diffusion graph contrastive learning model (RDGCL). We design our own GCN for CF based on both the diffusion, i.e., low-pass filter, and the reaction, i.e., high-pass filter, equations. Our proposed CL-based training occurs between reaction and diffusion-based embeddings, so there is no need for graph augmentations. Experimental evaluation on 6 benchmark datasets demonstrates that our proposed method outperforms state-of-the-art CL-based recommendation models. By enhancing recommendation accuracy and diversity, our method brings an advancement in CL for recommender systems.

1 INTRODUCTION

Contrastive learning (CL) is attracting much attention and is being actively researched in the field of machine learning [10, 35, 37, 44]. CL enhances the user/item embedding process with the learning representation principle, which increases the similarity between positive pairs and maximizes the dissimilarity between negative pairs. CL has achieved many successes in a variety of domains, including computer vision [8, 9, 29], natural language processing [2, 18, 56] and graph data [28, 55, 79, 80]. In the field of recommender systems, recent collaborative filtering (CF) methods are mostly based on it [3, 36, 41, 69, 73, 76, 77].

Integrating CL with graph convolutional networks (GCNs) has great potential for solving the data sparsity problem in recommender systems [36, 69]. GCN-based CF methods excel at capturing complex dependencies and interactions among entities in graph-structured data, making them suitable for modeling user-item interactions [6, 14, 16, 24, 30, 32, 33, 39, 40, 43, 46, 47, 59, 64]. However, the notorious data sparsity problem hinders the approach because most users only interact with a few items, and most items

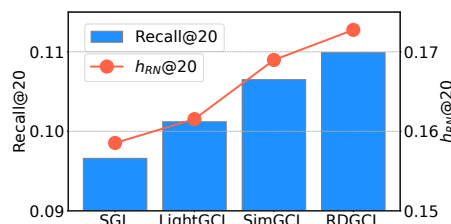


Figure 1: Comparison in terms of Recall@20 and $h_{RN}@20$, the harmonic mean of the recall and novelty (cf. Sec. 4.3), on Yelp. Our proposed model, RDGCL, outperforms recent CL-based methods, SGL, SimGCL, and LightGCL.

Table 1: Comparison of existing CL-based methods that differ at three points: i) how to generate views for CF, ii) using low-pass filters, and iii) using high-pass filters

Model	View generation	Low-pass filter	High-pass filter
SGL [69]	Node/edge dropout	✓	✗
SimGCL [76]	Injecting noises into embs.	✓	✗
LightGCL [3]	Filtering graphs with SVD	✓	✗
RDGCL	Low vs. High-pass embs.	Diffusion eq.	Reaction eq.

receive only a few interactions. By integrating CL into the GCN-based CF, one can let a model be exposed to more diverse training environments. While utilizing only the sparse interaction leads quickly to overfitting, this enhanced training mechanism greatly stabilizes the overall training process.

CL methods for existing recommender systems rely heavily on graph augmentation techniques to generate positive and negative pairs. These graph augmentation techniques involve perturbing graph structures (e.g., stochastic edge/node dropouts) or adding noises to the node embedding. As in Table 1, SGL [69] perturbs graph structures and then maximizes the representations’ consistency under different views. SimGCL [77], which says that it is not necessary to augment graph structures, injects uniform noises into embeddings to augment the node representation. It then learns node representations (embeddings) by maximizing the consistency

*Both authors contributed equally to this research.

[†]Noseong Park is the corresponding author.

between different graph augmentations. SimGCL has a disadvantage that one needs to manually adjust the noise magnitude. LightGCL [3] reconstructs graph structures through the singular value decomposition (SVD) but additional computational costs are incurred for SVD.

In general, the existing paradigm of CL-based CF has limitations. First, the graph augmentation brings noises and redundancies, which can degrade the quality of the learned node representation. Second, graph structure augmentations may not generate sufficient diversity and contrast among node representations (cf. Fig. 1). Third, these existing CL-based CF methods are all based on GCNs using only low-pass graph filters, e.g., LightGCN, and overlooked the importance of high-pass filters [14, 15]. Using only low-pass filter-based GCNs has a limitation in learning the node representation due to the notorious oversmoothing problem, i.e., node representations become similar to each other (cf. Sec. 4.7).

To address these limitations, the key design points in our proposed method are twofold: i) a new GCN-based network is proposed for CF, and ii) a new CL method for it is designed. Our method with the two contributions is called *reaction-diffusion graph contrastive learning* (RDGCL) since those design points are greatly inspired by the reaction-diffusion equation.

One can consider that the diffusion equation under the context of GCNs is for making neighboring nodes’ embeddings similar and the reaction equation is for making them dissimilar — another way of interpreting the equation is that the diffusion (resp. reaction) equation describes attractive (resp. repulsive) forces [14, 15, 21, 66]. In the perspective of graph signal processing, the diffusion (resp. reaction) equation corresponds to the low-pass (resp. high-pass) filter. We utilize the reaction-diffusion equation in the following ways in RDGCL:

- (1) We design our own GCN for CF based on both the diffusion, i.e., low-pass filter, and the reaction, i.e., high-pass filter, equations, whereas existing CL and GCN-based CF methods consider only the low-pass filter.
- (2) Our proposed CL-based training occurs between our network’s diffusion and reaction-based embeddings (cf. Fig. 3).

In addition, RDGCL differs from other CL-based CF methods in that it has a single pass. For instance, LightGCL has two GCN instances, one for the main CF task and the other for the augmented graph view purpose, which we call *two passes*. Since RDGCL has both the diffusion and the reaction layers internally, we can perform the CL training between them. This shows an efficient design choice in our method.

This paper presents a comprehensive set of evaluations with 6 benchmark datasets and 13 baselines. Our experimental results demonstrate the superiority of RDGCL in terms of the recommendation accuracy, coverage, and novelty. As shown in Fig. 1, RDGCL outperforms existing CL-based CF methods by large margins by accurately recalling more diverse items for recommendation. The main contributions of this paper are summarized as follows:

- We propose a novel approach called the reaction-diffusion graph contrastive learning (RDGCL) method for collaborative filtering, which uses both the diffusion equation for low-pass filtering and the reaction equation for high-pass

filtering in its neural network design and its CL training method.

- To our knowledge, RDGCL is the first to adopt the reaction-diffusion equation for CL-based collaborative filtering.
- RDGCL outperforms existing CF methods on 6 benchmark datasets.
- We improve performance with the most balanced model in terms of accuracy and diversity metrics (e.g., coverage and novelty).
- For reproducibility, our codes and data are available in the supplementary material.

2 PRELIMINARIES & RELATED WORK

2.1 Graph Filters and GCN-based CFs

Let $\mathbf{R} \in \{0, 1\}^{|\mathcal{U}| \times |\mathcal{V}|}$, where \mathcal{U} is a set of users and \mathcal{V} is a set of items, be an interaction matrix. $R_{u,v}$ is 1 iff an interaction (u, v) is observed in data, or otherwise 0. Let $\mathbf{A} \in \mathbb{R}^{N \times N}$ be the adjacency matrix, where $N = |\mathcal{U}| + |\mathcal{V}|$ is the number of nodes. \mathbf{L} is the Laplacian matrix of the graph, defined as $\mathbf{L} = \mathbf{D} - \mathbf{A} \in \mathbb{R}^{N \times N}$, where \mathbf{D} is the diagonal degree matrix. The symmetric normalized adjacency matrix is defined as $\tilde{\mathbf{A}} = \tilde{\mathbf{D}}^{-\frac{1}{2}} \tilde{\mathbf{A}} \tilde{\mathbf{D}}^{-\frac{1}{2}}$, where $\tilde{\mathbf{D}} = \mathbf{D} + \mathbf{I}$, where $\tilde{\mathbf{A}} = \mathbf{A} + \mathbf{I}$. The symmetric normalized Laplacian matrix is defined in a similar fashion: $\tilde{\mathbf{L}} = \mathbf{I} - \tilde{\mathbf{A}}$.

The operation of multiplying a graph signal \mathbf{x} by a Laplacian matrix $\tilde{\mathbf{L}}\mathbf{x}$ can be understood as a filter that modifies the magnitude of the components of \mathbf{x} in the frequency domain [19]. Each eigenvector \mathbf{v}_i of the Laplacian matrix aligns with a group of interconnected nodes in the graph.

The Laplacian filter enhances signal components aligned with basis functions associated with higher eigenvalues $\gamma_i \in (1, 2)$ while reducing those aligned with lower eigenvalues $\gamma_i \in [0, 1]$. Specifically, for clusters of nodes strongly aligned with \mathbf{v}_i and $\gamma_i > 1$, the projection $\gamma_i \mathbf{v}_i \mathbf{v}_i^\top \mathbf{x}$ amplifies the signal within the cluster, intensifying the variations among nodes in that cluster. In contrast, for larger clusters aligned with \mathbf{v}_i and $\gamma_i < 1$, the projection suppresses the signal within the cluster, leading to reduced differences among nodes in that cluster. Consequently, Laplacian matrices can be thought of as high-pass filters that emphasize differences in node features [22]. In contrast, the normalized adjacency matrix function as low-pass filters, diminishing non-smooth signal components [49]. This is due to all eigenvalues of adjacency matrices being less than 1, i.e., $\gamma_i \in (-1, 1]$.

While most GCN-based collaborative filtering (CF) approaches are constrained to employing low-pass filters, a prominent model in the field, LightGCN [30], has emerged. This model employs a linear GCN, functioning as a low-pass filter to enhance the smoothness of node representations, thereby becoming a standard choice for GCN-based CF. Some studies propose recommendation models using high-pass filters [14, 52, 60], but no studies use them to generate views in contrastive learning for recommendation. Therefore, our key idea is to apply a high-pass graph filter in the CL framework.

2.2 Contrastive Learning for Recommendation

Deep learning-based recommender systems have shown remarkable performance in recent years. However, they suffer from the

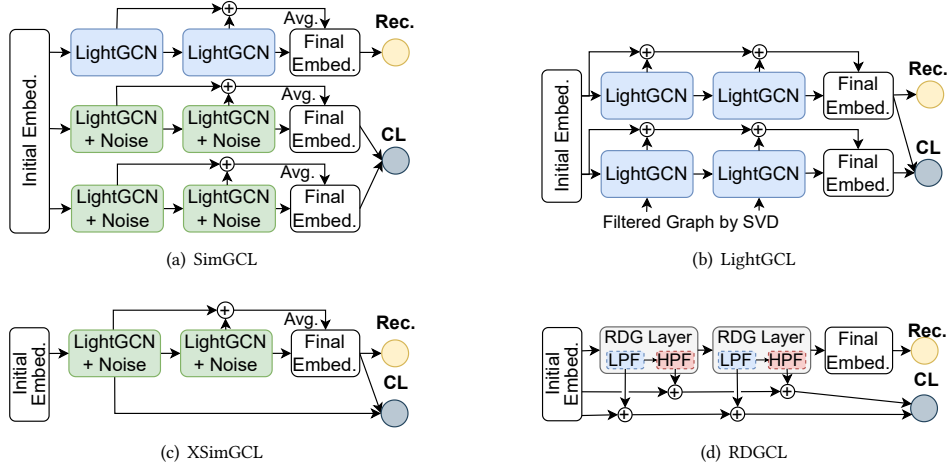


Figure 2: The architectures of SimGCL, LightGCL, XSimGCL, and RDGCL. In all methods, only the initial embeddings are trained and the graph convolutional layers do not have trainable parameters.

data sparsity and cold-start problems since they heavily rely on labels, i.e., positive user-item interactions [74, 75]. To address these problems, self-supervised-based recommendation methods have been proposed to extract useful information from unlabeled interactions [36, 69]. Especially, CL-based CF methods, which augment different views and contrast them to align node representations, show promising outcomes.

SGL [69] first applied the CL to graph-based recommendation, utilizing LightGCN [30] as its backbone encoder. It introduces three operators to generate augmented views: node dropouts, edge dropouts, and random walks. By contrasting these augmented views, it improves the recommendation accuracy, especially for long-tail items, and the robustness against interaction noises. For CL, InfoNCE [51] is defined as follows:

$$\mathcal{L}_{CL} = \sum_{i \in \mathcal{B}} -\log \frac{\exp(\text{sim}(\mathbf{e}'_i, \mathbf{e}''_i)/\tau)}{\sum_{j \in \mathcal{B}} \exp(\text{sim}(\mathbf{e}'_i, \mathbf{e}''_j)/\tau)}, \quad (1)$$

where i, j are a user and an item in a mini-batch \mathcal{B} respectively, $\text{sim}(\cdot)$ is the cosine similarity, τ is the temperature, and $\mathbf{e}', \mathbf{e}''$ are augmented node representations. The CL loss increases the alignment between the node representations of \mathbf{e}'_i and \mathbf{e}''_i nodes, viewing the representations of the same node i as positive pairs. Simultaneously, it minimizes the alignment between the node representations of \mathbf{e}'_i and \mathbf{e}''_j , viewing the representations of the different nodes i and j as negative pairs.

SimGCL [77] simplifies the graph augmentation process for its CL by perturbing node representations with random noises. XSimGCL [76] replaces the final-layer CL of SimGCL with a cross-layer CL approach – our RDGCL also follows this cross-layer CL approach. It only utilizes one GCN-based encoder and contrasts the embeddings of different layers, and this cross-layer CL reduces the computational complexity since it has only one neural network. LightGCL [3] proposes a singular value decomposition (SVD)-based graph augmentation strategy to effectively distill global collaborative signals. In specific, SVD is first performed on the adjacency

matrix. Then, the list of singular values is truncated to retain the largest values, i.e., the ideal low-pass filter, and then its truncated matrix is used to purify the adjacency matrix.

As shown in Fig. 2, existing CL-based recommender systems are limited to low-pass filters since i) their backbones are mostly LightGCN and ii) they augment views with low-pass filters.

2.3 Reaction-Diffusion Equations

Reaction-diffusion equations are partial differential equations that describe how the concentration of substances distributed in space changes under the influence of two processes: local chemical reactions and diffusion [38, 61]. In general, a reaction-diffusion equation can be written as

$$\frac{\partial u}{\partial t} = \nabla^2 u + R(u), \quad (2)$$

where $u(x, t)$ is the concentration of a substance at position x and time t , ∇^2 is the Laplace operator, and $R(u)$ is the reaction term. There are different types of reaction terms to describe pattern formation phenomena in various biological [25, 38, 42, 45], chemical [1, 53] systems, and image processing [11, 12, 20, 23, 48, 54, 58, 62, 63, 67, 68].

Reaction-diffusion equations on graphs can be discretized using finite difference methods. For example, using the explicit Euler scheme, we can approximate the reaction-diffusion equation under the context of graph signal processing as follows:

$$u(t + \Delta t) = u(t) + \Delta t(-\tilde{\mathcal{L}}u(t) + R(u(t))), \quad (3)$$

where Δt is the time step size and $u(t) \in \mathbb{R}^N$ is the graph signal at time t . This equation can be interpreted as updating the graph signal by applying the diffusion term and the reaction term at each time step. The diffusion term captures the tendency of the quantity to spread over the graph, while the reaction term accounts for the local interactions or transformations of the quantity at each node.

We design the interaction of nodes in this reaction term using the high-pass filter.

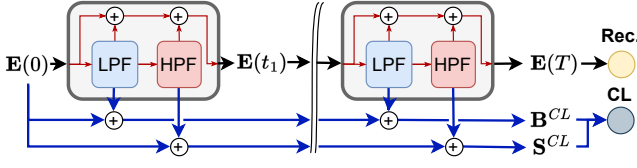


Figure 3: The illustration of our RDGCL where we solve our reaction-diffusion system with the explicit Euler method.

2.4 Neural Ordinary Differential Equations

Neural ordinary differential equations (NODEs) [7] solve the initial value problem (IVP), which involves a Riemann integral problem, to calculate $\mathbf{h}(t_{i+1})$ from $\mathbf{h}(t_i)$:

$$\mathbf{h}(t_{i+1}) = \mathbf{h}(t_i) + \int_{t_i}^{t_{i+1}} f(\mathbf{h}(t_i), t; \theta_f) dt, \quad (4)$$

where the neural network parameterized by θ_f approximates the time-derivative of \mathbf{h} , i.e., $\dot{\mathbf{h}} \stackrel{\text{def}}{=} \frac{d\mathbf{h}(t)}{dt}$. We rely on various ODE solvers to solve the integral problem, from the explicit Euler method to the 4th order Runge–Kutta (RK4) method. For instance, the Euler method is as follows:

$$\mathbf{h}(t+s) = \mathbf{h}(t) + s \cdot f(\mathbf{h}(t)), \quad (5)$$

where s is a pre-configured step size. Eq. (5) is identical to a residual connection when $s = 1$ and therefore, NODEs are a continuous generalization of residual networks.

3 PROPOSED METHOD

We describe our RDGCL which consists of a reaction-diffusion equation and a CL framework. We first review its overall architecture and then introduce details.

3.1 Overall Architecture

In Fig. 3, we show the overall architecture of RDGCL. The initial embedding $\mathbf{E}(0)$ is fed into the reaction-diffusion graph (RDG) layer. Then we have the embedding $\mathbf{E}(t)$ evolving over time $t \in [0, T]$. The embedding evolutionary process can be written as follows:

$$\mathbf{E}(T) = \mathbf{E}(0) + \int_0^T f(\mathbf{E}(t)) dt, \quad (6)$$

where $\mathbf{E}(t) \in \mathbb{R}^{N \times D}$ is the node embedding matrix at time t with D dimensions. $f(\mathbf{E}(t))$ is a RDG layer which outputs $\frac{d\mathbf{E}(t)}{dt}$.

As shown in Fig. 3, the iterative workflow of the RDG layer is as follows:

- (1) The RDG layer applies a low-pass filter (e.g., a diffusion process) to $\mathbf{E}(t_i)$ to derive its low-pass filtered embedding $\mathbf{B}(t_i)$,
- (2) It then applies a high-pass filter (e.g., a reaction process) to $\mathbf{B}(t_i)$ to derive $\mathbf{E}(t_{i+1})$.

RDGCL uses $\mathbf{E}(T)$ for the recommendation task while contrasting the two representations, \mathbf{B}^{CL} and \mathbf{S}^{CL} , each of which is the sum of the low-pass or high-pass information only. This approach called as *cross-layer CL* or *single-pass CL*.

3.2 Reaction-Diffusion Graph Layer

Our reaction-diffusion graph (RDG) layer can be written as the following equation and solved by the ODE solver:

$$f(\mathbf{E}(t)) := \frac{d\mathbf{E}(t)}{dt} = -\tilde{\mathbf{L}}\mathbf{E}(t) + \alpha R(\mathbf{E}(t)), \quad (7)$$

where $R(\cdot)$ is a reaction term, and α is a reaction rate coefficient to (de-)emphasize the reaction term. The reaction term corresponds to the high-pass filter in the perspective of graph signal processing.

3.2.1 Diffusion Process as Low-pass Filter. Multiplying with the adjacency matrix (\mathbf{A} or $\tilde{\mathbf{A}}$) can be regarded as a low-pass filtering operation. Many GCNs can be generalized to the following diffusion process [4, 13, 26, 34, 49, 65]:

$$\mathbf{B}(t) = \mathbf{E}(t) - \tilde{\mathbf{L}}\mathbf{E}(t) = \mathbf{E}(t) + (\tilde{\mathbf{A}} - \mathbf{I})\mathbf{E}(t) = \tilde{\mathbf{A}}\mathbf{E}(t). \quad (8)$$

3.2.2 Reaction Process as High-pass Filter. The reaction process is designed to act as a high-pass filter. Multiplying with the Laplacian matrix (\mathbf{L} or $\tilde{\mathbf{L}}$) can be regarded as a high-pass filter [22]. We apply it to $\mathbf{B}(t)$ as follows:

$$R(\mathbf{E}(t)) := \tilde{\mathbf{L}}\mathbf{B}(t) = \tilde{\mathbf{L}}(\tilde{\mathbf{A}}\mathbf{E}(t)). \quad (9)$$

We emphasize that the embedding made from the reaction process is not independent from it from the diffusion process since we apply the reaction process to $\mathbf{B}(t)$ and therefore, our contrastive learning, which will be described layer, addresses the potential sparsity issues in $\mathbf{B}(t)$ and $R(\mathbf{E}(t))$.

3.3 Cross-layer Contrastive Learning

We extract the low-pass (or diffusion) and the high-pass (or reaction) views from Eq. (7) along the time domain $[0, T]$ as follows:

$$\mathbf{B}^{CL} = \mathbf{E}(0) + \sum_{i=1}^K \mathbf{B}(t_i), \quad \mathbf{S}^{CL} = \mathbf{E}(0) + \sum_{i=1}^K R(\mathbf{E}(t_i)), \quad (10)$$

where we solve Eq. (6) via K steps with an ODE solver.

After generating the diffusion and reaction views, we employ a contrastive objective that enforces the filtered representations of each node in the two views to agree with each other. We perform the CL training by directly contrasting the reaction’s augmented view \mathbf{S}^{CL} with the diffusion’s view \mathbf{B}^{CL} using InfoNCE [51] loss:

$$\mathcal{L}_{CL} = \sum_{i \in \mathcal{B}} -\log \frac{\exp(\text{sim}(\mathbf{b}_i^{CL}, \mathbf{s}_i^{CL})/\tau)}{\sum_{j \in \mathcal{B}} \exp(\text{sim}(\mathbf{b}_i^{CL}, \mathbf{s}_j^{CL})/\tau)}, \quad (11)$$

where i, j are a user and an item in a sampled batch \mathcal{B} , and \mathbf{b}_i^{CL} , \mathbf{s}_i^{CL} , and \mathbf{s}_j^{CL} are node representations from Eq. (10).

As shown in Eq. (12), therefore, our joint learning objective is as follows:

$$\mathcal{L} = \mathcal{L}_{BPR} + \lambda_1 \cdot \mathcal{L}_{CL} + \lambda_2 \cdot \|\Theta\|_2^2, \quad (12)$$

which consists of the Bayesian personalized ranking (BPR) loss \mathcal{L}_{BPR} and the CL loss \mathcal{L}_{CL} . The hyperparameters λ_1 and λ_2 control the trade-off among the two losses and the regularization term. Θ denotes the embeddings to learn, i.e., $\Theta = \mathbf{E}(0)$ in our framework.

After minimizing the joint loss in Eq. (12), we use the output of the RDG layer, i.e., $\mathbf{E}(T)$, as the final representation. The exact training method is described in Alg. 1.

Algorithm 1: CL with Reaction-Diffusion Graph Layers

Input: Interaction matrix R

```

1 Initialize  $E(0)$ ;
2  $m \leftarrow 0$ ;
3 while  $m < max\_iter$  do
4   Solve Eq. (6) from  $E(0)$ ;
5   Generate  $B^{CL}$  and  $S^{CL}$  with Eq. (10);
6   Compute the joint objective  $\mathcal{L}$  with Eq. (12);
7   Update  $E(0)$  to minimize  $\mathcal{L}$ ;
8    $m \leftarrow m + 1$ ;
9 return  $E(0)$ ;

```

Table 2: The comparison of analytical time complexity

Component	LightGCN	SGL	SimGCL	RDGCL
Adj. Matrix	$\mathcal{O}(2 A)$	$\mathcal{O}((2+4\rho) A)$	$\mathcal{O}(2 A)$	$\mathcal{O}(2 A)$
GCN	$\mathcal{O}(2 A KD)$	$\mathcal{O}((2+4\rho) A KD)$	$\mathcal{O}(6 A KD)$	$\mathcal{O}(4 A KD)$
CL	N/A	$\mathcal{O}(\mathcal{B} MD)$	$\mathcal{O}(\mathcal{B} MD)$	$\mathcal{O}(\mathcal{B} MD)$

3.4 Relationship to Existing Models

Comparison to CL-based methods. RDGCL uses a single unified pass for the CL task and the CF task while SimGCL and LightGCL use separate passes for the two different tasks. This makes RDGCL more efficient and consistent in learning representations. XSimGCL is similar to RDGCL in that it is designed with as single pass using a cross-layer CL method, but is still confined to low-pass filters only. RDGCL adopts the reaction-diffusion system to contrast the information from the different graph signals. However, SimGCL and LightGCL perform the CL training for their final embeddings only, overlooking their intermediate embeddings. This enables RDGCL to capture more diverse and complementary features from the graph structure. The main difference between RDGCL and these methods is that RDGCL uses the reaction-diffusion-based system to generate embeddings, instead of the noise injection, the edge/node drop, which can capture more fine-grained information from different graph frequency domains – note that the diffusion (resp. reaction) system corresponds to the low-pass (resp. high-pass) graph filter.

Comparison to differential equation-based methods. LT-OCF is a continuous-time generalization of LightGCN. If the reaction term of RDGCL is removed and its CL is not used, RDGCL reduces to LT-OCF. BSPM is yet another CF method which uses the diffusion and the reaction systems separately. It first applies its diffusion process directly to the interaction matrix R without learning embeddings and then separately apply the reaction process to the diffusion outcome – GF-CF also applies a graph signal process method directly to R . Therefore, BSPM does not follow Eq. (7) where the diffusion and the reaction processes happens at the same time.

3.5 Model Complexity

This section analyzes the time complexity of RDGCL and compares it with the baselines, LightGCN, SGL, and SimGCL. We discuss the time complexity within a single batch. We define $|A|$ as the edge numbers, $|\mathcal{B}|$ denotes the batch size, M represents the node numbers in a batch, K is the number of layers (resp. ODE steps) in

Table 3: Statistics of datasets

Dataset	#Users	#Items	#Interactions	Density
Yelp	29,601	24,734	1,374,594	0.188%
Gowalla	50,821	57,440	1,302,695	0.045%
Amazon-Books	78,578	77,801	2,880,201	0.047%
Amazon-Electronics	1,435	1,522	35,931	1.645%
Amazon-CDs	43,169	35,648	777,426	0.051%
Tmall	47,939	41,390	2,619,389	0.132%

baselines (resp. RDGCL), and ρ denotes the edge keeping-rate in SGL. Table 2 summarizes the time complexity which tells us the following findings:

- LightGCN, SimGCL, and RDGCL do not need to perform graph augmentation but only require the time complexity of $\mathcal{O}(2|A|)$ to construct the adjacency matrix. In contrast, SGL requires nearly three times the cost because it needs to perform the graph augmentation twice.
- SGL requires three forward computations on the original graph and the two subgraphs in a graph convolution step. So, the time cost is almost three times that of LightGCN. RDGCL requires only two matrix multiplication operations in Eq. (7), reducing the computational cost in a step.
- For the CL loss computation, the complexity of RDGCL is the same as those of other models, which is $\mathcal{O}(|\mathcal{B}|D + |\mathcal{B}|MD)$, where $\mathcal{O}(|\mathcal{B}|D)$ and $\mathcal{O}(|\mathcal{B}|MD)$ are for positive and negative views, respectively. For brevity, we show it as $\mathcal{O}(|\mathcal{B}|MD)$.

4 EXPERIMENTS

In this section, we describe our experimental environments and results. The following software and hardware environments were used for all experiments: UBUNTU 18.04 LTS, PYTORCH 1.9.0, TORCHDISTRIBUTION 0.2.2, CUDA 11.3, i9 CPU, and RTX 3090.

4.1 Experimental Environments

4.1.1 Datasets and Baselines. We evaluate our model and baselines with 6 real-world benchmark datasets: Yelp, Gowalla, Amazon-Books, Amazon-Electronics, Amazon-CDs, and Tmall [6, 27, 30, 64]. We summarize the dataset statistics in Table 3. We compare our model with the following 13 baselines with diverse technical characteristics:

- (1) Graph-based CFs include LightGCN [30], LT-OCF [16], HML-LET [39], GF-CF [59], and BSPM [14];
- (2) Graph CL methods for other tasks include SimGRACE [70] and GCA [80];
- (3) Hypergraph-based CFs include HCCF [71] and SHT [72];
- (4) Graph CL methods for CF include SGL [69], SimGCL [77], XSimGCL [76], and LightGCL [3].

4.1.2 Evaluation Protocols and Hyperparameters. We use the widely used ranking metrics: Recall@20/40 and NDCG@20/40. For Yelp, Gowalla, and Amazon-Books, we reuse the train/valid/test splits taken from Cai et al. [3]. For Amazon-Electronics and Amazon-CDs, we use the dataset settings used by Mao et al. [47]. We also further

Table 4: Performance comparison to popular graph-based CF and CL models. We highlight the best three results in red (first), blue (second), and purple (third). *Imp.* stands for relative improvement over second-best performance.

Data	Metric	LightGCN	LT-OCF	HMLET	SGL	SimGRACE	GCA	HCCF	SHT	SimGCL	XSimGCL	LightGCL	GF-CF	BSPM	RDGCL	<i>Imp.</i>
Yelp	Recall@20	0.0826	0.0947	0.0859	0.0967	0.0899	0.0779	0.0995	0.0853	0.1065	0.0974	0.1012	0.1043	0.1059	0.1099	3.19%
	NDCG@20	0.0690	0.0800	0.0699	0.0824	0.0775	0.0670	0.0842	0.0719	0.0912	0.0823	0.0870	0.0890	0.0913	0.0939	2.77%
	Recall@40	0.1346	0.1531	0.1388	0.1544	0.1443	0.1279	0.1578	0.1382	0.1688	0.1564	0.1591	0.1659	0.1677	0.1721	1.95%
	NDCG@40	0.0882	0.1016	0.0898	0.0906	0.1032	0.0851	0.1056	0.0913	0.1038	0.1040	0.1081	0.1115	0.1139	0.1165	2.28%
Gowalla	Recall@20	0.1294	0.2215	0.2157	0.2371	0.1519	0.1899	0.2222	0.1877	0.2304	0.2314	0.2351	0.2347	0.2455	0.2564	4.43%
	NDCG@20	0.0781	0.1287	0.1270	0.1400	0.0850	0.1100	0.1298	0.1119	0.1363	0.1380	0.1386	0.1382	0.1472	0.1549	5.19%
	Recall@40	0.1869	0.3131	0.3010	0.3269	0.2225	0.2690	0.3106	0.2671	0.3195	0.3224	0.3251	0.3266	0.3342	0.3460	3.53%
	NDCG@40	0.0932	0.1529	0.1494	0.1636	0.1034	0.1309	0.1528	0.1325	0.1597	0.1619	0.1622	0.1624	0.1707	0.1783	4.45%
Amazon-Books	Recall@20	0.0950	0.0987	0.0934	0.1333	0.0982	0.0850	0.1187	0.0834	0.1317	0.1148	0.1356	0.1392	0.1377	0.1416	1.74%
	NDCG@20	0.0704	0.0734	0.0697	0.1081	0.0769	0.0668	0.0912	0.0630	0.1042	0.0887	0.1081	0.1158	0.1171	0.1141	-2.56%
	Recall@40	0.1454	0.1512	0.1417	0.1848	0.1429	0.1248	0.1728	0.1296	0.1867	0.1692	0.1917	0.1893	0.1830	0.1979	3.22%
	NDCG@40	0.0872	0.0910	0.0858	0.1249	0.0905	0.0799	0.1090	0.0782	0.1221	0.1065	0.1264	0.1321	0.1316	0.1324	0.23%
Amazon-Electronics	Recall@20	0.1251	0.1319	0.1258	0.1331	0.1236	0.1254	0.0597	0.0909	0.1371	0.1295	0.1306	0.1306	0.1311	0.1393	1.60%
	NDCG@20	0.0737	0.0792	0.0755	0.0783	0.0712	0.0727	0.0338	0.0912	0.0777	0.0748	0.0771	0.0771	0.0792	0.0809	2.15%
	Recall@40	0.1842	0.1850	0.1828	0.1913	0.1811	0.1306	0.0918	0.1409	0.1939	0.1833	0.1907	0.1907	0.1742	0.1982	2.22%
	NDCG@40	0.0896	0.0933	0.0908	0.0942	0.0868	0.0771	0.0426	0.0640	0.0934	0.0897	0.0934	0.0934	0.0912	0.0972	3.18%
Amazon-CDs	Recall@20	0.0956	0.1572	0.1438	0.1565	0.0729	0.0941	0.0658	0.1256	0.1583	0.1335	0.1460	0.1394	0.1443	0.1622	2.46%
	NDCG@20	0.0561	0.0981	0.0900	0.0997	0.0434	0.0581	0.0434	0.0756	0.1020	0.0804	0.0925	0.0912	0.0929	0.1054	3.33%
	Recall@40	0.1484	0.2196	0.2011	0.2159	0.1150	0.1346	0.1076	0.1829	0.2183	0.1952	0.2038	0.1940	0.1974	0.2225	1.92%
	NDCG@40	0.0708	0.1157	0.1061	0.1163	0.0552	0.0695	0.0542	0.0919	0.1188	0.0975	0.1086	0.1066	0.1085	0.1223	2.95%
Tmall	Recall@20	0.0717	0.0737	0.0676	0.1035	0.0705	0.0730	0.0930	0.0706	0.0993	0.0880	0.1033	0.0879	0.0879	0.1040	0.44%
	NDCG@20	0.0498	0.0515	0.0464	0.0745	0.0488	0.0511	0.0663	0.0492	0.0712	0.0626	0.0626	0.0612	0.0612	0.0753	0.64%
	Recall@40	0.1126	0.1168	0.1059	0.1545	0.1104	0.1124	0.1427	0.1118	0.1505	0.1370	0.1370	0.1379	0.1380	0.1559	0.86%
	NDCG@40	0.0640	0.0665	0.0598	0.0922	0.0626	0.0648	0.0834	0.0634	0.0890	0.0795	0.0795	0.0784	0.0785	0.0933	0.85%

search the best hyperparameters for baselines based on their recommended hyperparameters. For our method, we test the following hyperparameters:

- For solving the integral problem, we consider the following ODE solvers: the Euler method and RK4. However, we found that Euler and RK4 produce almost the same results in our preliminary experiments, so we test only the Euler method;
- The number of steps K is in $\{1, 2, 3\}$, and the terminal time T is in $\{1.0, 1.1, \dots, 3.0\}$;
- The reaction rate coefficient α is in $\{0.1, \dots, 1.0\}$;
- The size of embedding D is in $\{64, 128, 256\}$;
- The learning rate is in $\{1.0 \times 10^{-5}, 1.0 \times 10^{-4}, 1.0 \times 10^{-3}, 1.0 \times 10^{-2}\}$;
- The regularization weight for the InfoNCE loss λ_1 is in $\{0.1, 0.2, \dots, 1.0\}$;
- The regularization weight λ_2 is in $\{1.0 \times 10^{-8}, 1.0 \times 10^{-7}, 1.0 \times 10^{-6}, 1.0 \times 10^{-5}\}$.

The best configuration set in each data is as follows: In Yelp, $K = 2$, $T = 2$, $\alpha = 0.6$, $\tau = 0.1$, and $\lambda_1 = 0.3$. In Gowalla, $K = 2$, $T = 2$, $\alpha = 0.2$, $\tau = 0.4$, and $\lambda_1 = 0.5$. In Amazon-Books, $K = 2$, $T = 2$, $\alpha = 0.8$, $\tau = 0.1$, and $\lambda_1 = 0.2$. In Amazon-Electronics, $K = 2$, $T = 2$, $\alpha = 0.2$, $\tau = 1.0$, and $\lambda_1 = 0.2$. In Amazon-CDs, $K = 2$, $T = 2$, $\alpha = 0.1$, $\tau = 0.2$, and $\lambda_1 = 0.2$. In Tmall, $K = 2$, $T = 2$, $\alpha = 0.6$, $\tau = 0.2$, and $\lambda_1 = 0.5$.

4.2 Experimental Results

In Table 4, we summarize the overall accuracy in terms of Recall@20/40 and NDCG@20/40. As reported, our method clearly shows the highest accuracy in most cases. Specifically for Gowalla, RDGCL's NDCG@20 is 5.19% higher than the best baseline.

SGL and SimGCL work well in some cases, and only SimGCL is comparable to our method for Amazon-Electronics and Amazon-CDs. However, the accuracy gap between our method and SimGCL is still non-trivial. For Tmall, SGL shows higher accuracies than SimGCL, and for Yelp, SimGCL outperforms SGL and LightGCL. LightGCL shows good performance for Amazon-Books. XSimGCL, known to be surprisingly efficient and performs well, does not perform the best on benchmark datasets we use.

To further verify the outstanding performance of RDGCL, we compare it with two other recently proposed graph-based recommendation methods. GF-CF and BSPM show excellent performance, occupying the 2nd and 3rd places, except for Tmall. Except for Amazon-Books, however, RDGCL beats both models in all metrics. In terms of NDCG@20, BSPM and GF-CF slightly outperform RDGCL on Amazon-Books. However, no existing methods are comparable to our proposed method across all datasets. Therefore, we believe that the concept of RDGCL proposed by us opens a new direction for CF.

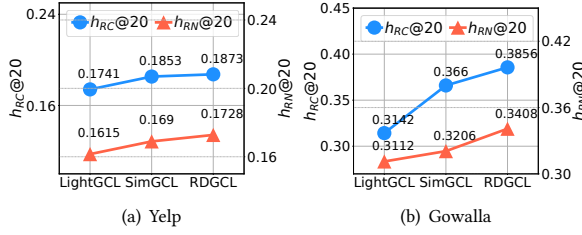


Figure 4: Trade-off among the three metrics on Yelp and Gowalla

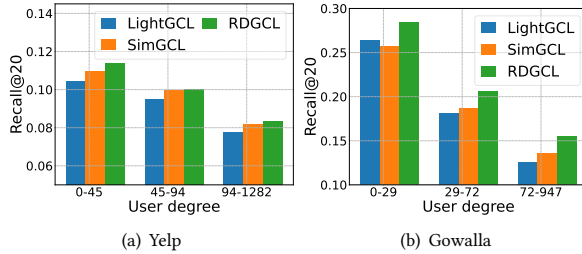


Figure 5: Performance on users of different sparsity degrees

4.3 Trade-off Among Recall, Coverage, and Novelty

We analyze the balanced nature of our model in terms of the recall, coverage, and novelty. We use the following two harmonic means:

$$h_{RC}@k = \frac{2 \times \text{Recall}@k \times \text{Coverage}@k}{\text{Recall}@k + \text{Coverage}@k}, \quad (13)$$

$$h_{RN}@k = \frac{2 \times \text{Recall}@k \times \text{Novelty}@k}{\text{Recall}@k + \text{Novelty}@k}, \quad (14)$$

where the coverage [14, 31] refers to the range of items that models can recommend, and the novelty [14, 78] measures how much unexpected the recommended items are in comparison with their global popularity. Via the two metrics, we can grasp a broader understanding of the impact of our proposed design.

As shown in Fig. 4, LightGCL, which is limited to low-pass filters, has low $h_{RC}@20$ and $h_{RN}@20$, while RDGCL has the highest balanced performance. In the case of SimGCL, both metrics are slightly lower than ours. This result suggests that RDGCL is the balanced design with improved accuracy and diversity.

4.4 Robustness to Sparsity and Popularity Bias

To measure the robustness for sparse user groups, we divide users into three groups and measure Recall@20 for each group. The users were classified into three groups by interaction degree: the bottom 80%, from the bottom 80% to 95%, and the top 5%. As shown in Fig. 5, RDGCL consistently outperforms the other baselines for all groups of users. Specifically, RDGCL shows good accuracy for extremely sparse user groups (<29) in Gowalla.

Furthermore, we study the robustness to the item popularity bias with our method and the baselines. Similarly to sparsity analysis, we divide items into three groups based on their degree of interaction

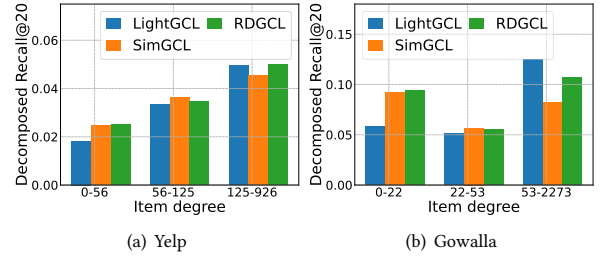


Figure 6: RDGCL’s ability to mitigate the popularity bias

Table 5: Ablation study on RDGCL

Model	Yelp		Gowalla	
	Recall@20	NDCG@20	Recall@20	NDCG@20
RDGCL	0.1099	0.0939	0.2564	0.1549
RDGCL-EB	0.1024	0.0871	0.2495	0.1524
RDGCL-ES	0.1094	0.0935	0.2531	0.1530

and measure Recall@20 on each group g . Following SGL [69], we use the decomposed Recall@ k , defined as follows:

$$\text{Recall}@k^{(g)} = \frac{|(I_{rec}^u)^{(g)} \cap I_{test}^u|}{|I_{test}^u|}, \quad (15)$$

where I_{rec}^u represents the candidate items in the top- k recommendation list and I_{test}^u represents the relevant items in the testing set for user u .

Fig. 6 shows that the accuracy of our model is higher for the item group with a low interaction degree compared to other baselines. This indicates that our model recommends long-tail items and has the ability to alleviate popularity bias.

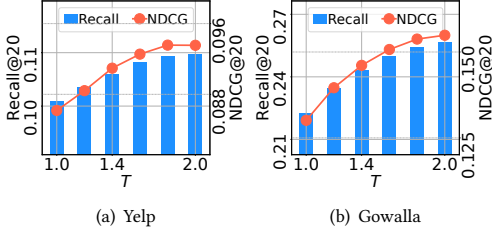
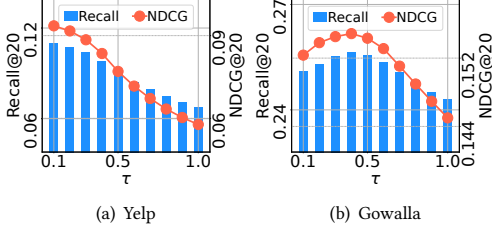
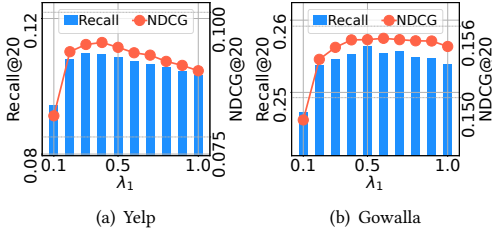
4.5 Ablation Study

As ablation study models, we define the following two models: i) the first ablation model contrasts $E(T)$ and B^{CL} , and ii) the second ablation model contrasts $E(T)$ and S^{CL} . The first (resp. second) model is denoted as “RDGCL-EB” (resp. “RDGCL-ES”) in the tables. In all cases, the ablation study model with $E(T)$ and S^{CL} significantly outperforms that with $E(T)$ and B^{CL} , e.g., Recall@20 of 0.1094 in Yelp by RDGCL-ES vs. 0.1024 by RDGCL-EB. However, RDGCL, which contrasts B^{CL} and S^{CL} , outperforms them. This shows that we need to perform the CL training between B^{CL} and S^{CL} to achieve the best model accuracy.

4.6 Sensitivity Analyses

In this section, we report the sensitivity of our model to some selected key hyperparameters: the terminal integral time T , the temperature τ , and the regularization weight for the InfoNCE loss λ_1 . If a hyperparameter is not reported in this subsection, it indicates that our model is not significantly sensitive to it.

4.6.1 Sensitivity to T . We test our model by varying T of the reaction-diffusion process, and the results are shown in Fig. 7. T close to 2 yields good outcomes for both Yelp and Gowalla.

Figure 7: Sensitivity on T Figure 8: Sensitivity on τ Figure 9: Sensitivity on λ_1

4.6.2 Sensitivity to τ . We test our model for various settings of τ , and the results are shown in Fig. 8. In Gowalla, the performance improves as the value of τ increases until reaching out an optimal point around 0.4. As τ becomes too large (e.g., $\tau \geq 0.5$), the performance decreases drastically in both datasets.

4.6.3 Sensitivity to λ_1 . We vary the regularization weight for the InfoNCE loss, denoted λ_1 . The results are shown in Fig. 9. For both Yelp and Gowalla, our method’s performance increases rapidly as λ_1 increases. After that, it shows slight decreases. However, the performance does not decrease as much as that of Fig. 8.

4.7 Empirical Evaluations for Oversmoothing

For our proposed method and existing graph-based methods, we analyze the oversmoothing phenomenon [17, 49, 50, 57]. The oversmoothing problem refers to the exponential convergence of all user/item node feature similarities towards the same constant value as the number of GCN layers increases – in this definition, it is important to use appropriate node similarity metrics. Since the commonly used mean-average distance (MAD) [5] is not an appropriate node similarity metric [57], we do not use MAD. However,

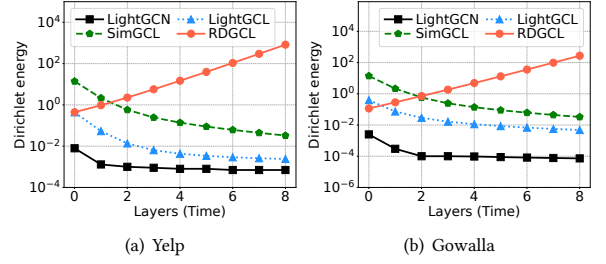


Figure 10: Evolution of the Dirichlet energy

Table 6: Efficiency comparison, w.r.t. the average training time per epoch

Model	Yelp	Gowalla	Amazon-Books	Amazon-Electronics	Amazon-CDs	Tmall
SGL	44.91s	44.48s	128.35s	19.58s	0.26s	102.55s
SimGCL	29.13s	50.02s	137.85s	17.46s	0.25s	154.08s
XSimGCL	20.40s	38.37s	110.75s	14.45s	0.21s	89.05s
LightGCL	19.94s	34.61s	117.37s	11.81s	0.20s	90.59s
RDGCL	22.54s	39.45s	121.67s	15.14s	0.20s	120.44s

the Dirichlet energy fulfills all the requirements of node similarity [57], so our approach to measure the oversmoothing is based on the Dirichlet energy on graphs as follows:

$$\mathcal{E}(\mathbf{E}) = \frac{1}{N} \sum_{i \in \mathcal{U} \cup \mathcal{V}} \sum_{j \in \mathcal{N}_i} \|\mathbf{E}_i - \mathbf{E}_j\|_2^2, \quad (16)$$

where \mathcal{N}_i is a one-hop neighborhood of a user/item node i .

We calculate the Dirichlet energy of the final embeddings that are used for recommendation by various methods. As shown in Fig. 10, RDGCL’s Dirichlet energy does not decrease even when the number of layers is high, whereas existing methods’ energies quickly decrease. As mentioned earlier, this is because existing methods are based only on low-pass filters, which shows the efficacy of our proposed reaction-diffusion equation-based method.

4.8 Empirical Runtime Complexity

We also report our actual running time during training in Table 6. Our method does not involve augmentations on graph structures, and its single pipeline for CL is not separated from the main channel unlike SGL and SimGCL. Thus, our training time is faster than theirs. However, it’s comparable and not as fast as XSimGCL and LightGCL. XSimGCL is faster than SimGCL because it only performs the graph convolution of LightGCN in one framework, but it does not outperform our method on all datasets. RDGCL runs marginally longer than XSimGCL and LightGCL because it performs the high-pass filter in the reaction term. Nevertheless, our proposed method is still effective since it outperforms both XSimGCL and LightGCL by large margins in the accuracy.

5 CONCLUSION & FUTURE WORK

In conclusion, we presented a novel approach called RDGCL for CF. It uses both the diffusion equation for low-pass filtering and

the reaction equation for high-pass filtering in its design and CL training method. To our knowledge, RDGCL is the first to adopt the reaction-diffusion equation for the CL-based CF. We demonstrated that RDGCL outperforms 13 baseline models on 6 benchmark datasets and achieves the best-balanced performance among the recall, coverage, and novelty. Our findings demonstrate the effectiveness of using high-pass filters and self-supervised signals and the potential as an alternative approach for recommender systems. Our work opens up new avenues for future research on investigating other filters and contrastive views and extending our method to other domains that can benefit from graph representation learning.

REFERENCES

- [1] Samuel M Allen and John W Cahn. 1979. A microscopic theory for antiphase boundary motion and its application to antiphase domain coarsening. *Acta metallurgica* 27, 6 (1979), 1085–1095.
- [2] Markus Bayer, Marc-André Kaufhold, and Christian Reuter. 2022. A survey on data augmentation for text classification. *Comput. Surveys* 55, 7 (2022), 1–39.
- [3] Xuheng Cai, Chao Huang, Lianghao Xia, and Xubin Ren. 2023. LightGCL: Simple Yet Effective Graph Contrastive Learning for Recommendation. In *ICLR*.
- [4] Benjamin Paul Chamberlain, James Rowbottom, Maria Goronova, Stefan Webb, Emanuele Rossi, and Michael M Bronstein. 2021. GRAND: Graph Neural Diffusion. In *ICML*.
- [5] Deli Chen, Yankai Lin, Wei Li, Peng Li, Jie Zhou, and Xu Sun. 2020. Measuring and relieving the over-smoothing problem for graph neural networks from the topological view. In *AAAI*, Vol. 34. 3438–3445.
- [6] Lei Chen, Le Wu, Richang Hong, Kun Zhang, and Meng Wang. 2020. Revisiting Graph Based Collaborative Filtering: A Linear Residual Graph Convolutional Network Approach. In *AAAI*.
- [7] Ricky T. Q. Chen, Yulia Rubanova, Jesse Bettencourt, and David K Duvenaud. 2018. Neural Ordinary Differential Equations. In *NeurIPS*.
- [8] Ting Chen, Simon Kornblith, Mohammad Norouzi, and Geoffrey Hinton. 2020. A simple framework for contrastive learning of visual representations. In *ICML*. PMLR, 1597–1607.
- [9] Ting Chen, Simon Kornblith, Kevin Swersky, Mohammad Norouzi, and Geoffrey Hinton. 2020. Big Self-Supervised Models are Strong Semi-Supervised Learners. *arXiv preprint arXiv:2006.10029* (2020).
- [10] Ting Chen, Calvin Luo, and Lala Li. 2021. Intriguing properties of contrastive losses. *NeurIPS* 34 (2021), 11834–11845.
- [11] Yunjin Chen and Thomas Pock. 2016. Trainable nonlinear reaction diffusion: A flexible framework for fast and effective image restoration. *IEEE transactions on pattern analysis and machine intelligence* 39, 6 (2016), 1256–1272.
- [12] Yunjin Chen, Wei Yu, and Thomas Pock. 2015. On learning optimized reaction diffusion processes for effective image restoration. In *CVPR*. 5261–5269.
- [13] Hwangyong Choi, Jeongwhan Choi, Jeehyun Hwang, Kookjin Lee, Dongeun Lee, and Noseong Park. 2023. Climate modeling with neural advection-diffusion equation. *Knowledge and Information Systems* 65, 6 (2023), 2403–2427.
- [14] Jeongwhan Choi, Seoyoung Hong, Noseong Park, and Sung-Bae Cho. 2023. Blurring-Sharpener Process Models for Collaborative Filtering. In *SIGIR*.
- [15] Jeongwhan Choi, Seoyoung Hong, Noseong Park, and Sung-Bae Cho. 2023. GREAT: Graph Neural Reaction-Diffusion Networks. In *ICML*.
- [16] Jeongwhan Choi, Jinsung Jeon, and Noseong Park. 2021. LT-OCF: Learnable-Time ODE-based Collaborative Filtering. In *CIKM*.
- [17] Jeongwhan Choi, Hyowon Wi, Jayoung Kim, Yehjin Shin, Kookjin Lee, Nathaniel Trask, and Noseong Park. 2023. Graph Convolutions Enrich the Self-Attention in Transformers! *arXiv preprint arXiv:2312.04234* (2023).
- [18] Yung-Sung Chuang, Rumen Dangovski, Hongyin Luo, Yang Zhang, Shiyu Chang, Marin Soljacic, Shang-Wen Li, Wen-tau Yih, Yoon Kim, and James Glass. 2022. DiffCSE: Difference-based Contrastive Learning for Sentence Embeddings. In *NAACL*.
- [19] Fan RK Chung. 1997. *Spectral graph theory*. Vol. 92. American Mathematical Soc.
- [20] G-H Cottet and L Germain. 1993. Image processing through reaction combined with nonlinear diffusion. *mathematics of computation* (1993), 659–673.
- [21] Francesco Di Giovanni, James Rowbottom, Benjamin P Chamberlain, Thomas Markovich, and Michael M Bronstein. 2022. Graph neural networks as gradient flows. *arXiv preprint arXiv:2206.10991* (2022).
- [22] Venkatesan N. Ekambaram. 2013. Graph Structured Data Viewed Through a Fourier Lens. *University of California, Berkeley* (2013).
- [23] Julio Esclarin and Luis Alvarez. 1997. Image quantization using reaction-diffusion equations. *SIAM J. Appl. Math.* 57, 1 (1997), 153–175.
- [24] Wenqi Fan, Xiaorui Liu, Wei Jin, Xiangyu Zhao, Jiliang Tang, and Qing Li. 2022. Graph Trend Filtering Networks for Recommendation. In *SIGIR*. 112–121.
- [25] Ronald Aylmer Fisher. 1937. The wave of advance of advantageous genes. *Annals of eugenics* 7, 4 (1937), 355–369.
- [26] William L. Hamilton. 2020. Graph Representation Learning. *Synthesis Lectures on Artificial Intelligence and Machine Learning* 14, 3 (2020), 1–159.
- [27] F Maxwell Harper and Joseph A Konstan. 2015. The movielens datasets: History and context. *Acm transactions on interactive intelligent systems (tiis)* 5, 4 (2015), 1–19.
- [28] Kaveh Hassani and Amir Hosein Khasahmadi. 2020. Contrastive multi-view representation learning on graphs. In *ICML*. PMLR, 4116–4126.
- [29] Kaiming He, Haoqi Fan, Yuxin Wu, Saining Xie, and Ross Girshick. 2020. Momentum contrast for unsupervised visual representation learning. In *CVPR*. 9729–9738.
- [30] Xiangnan He, Kuan Deng, Xiang Wang, Yan Li, YongDong Zhang, and Meng Wang. 2020. LightGCN: Simplifying and Powering Graph Convolution Network for Recommendation. In *SIGIR*.
- [31] Jonathan L. Herlocker, Joseph A. Konstan, Loren G. Terveen, and John T. Riedl. 2004. Evaluating Collaborative Filtering Recommender Systems. *ACM Trans. Inf. Syst.* 22, 1 (2004), 5–53.
- [32] Seoyoung Hong, Minju Jo, Seungji Kook, Jaeun Jung, Hyowon Wi, Noseong Park, and Sung-Bae Cho. 2022. TimeKit: A Time-series Forecasting-based Upgrade Kit for Collaborative Filtering. In *2022 IEEE International Conference on Big Data (Big Data)*. IEEE, 565–574.
- [33] Jun Hu, Shengsheng Qian, Quan Fang, and Changsheng Xu. 2022. MGDCF: Distance Learning via Markov Graph Diffusion for Neural Collaborative Filtering. *arXiv preprint arXiv:2204.02338* (2022).
- [34] Jeehyun Hwang, Jeongwhan Choi, Hwangyong Choi, Kookjin Lee, Dongeun Lee, and Noseong Park. 2021. Climate modeling with neural diffusion equations. In *ICDM*. IEEE, 230–239.
- [35] Ashish Jaiswal, Ashwin Ramesh Babu, Mohammad Zaki Zadeh, Debapriya Banerjee, and Fillia Makedon. 2020. A survey on contrastive self-supervised learning. *Technologies* 9, 1 (2020), 2.
- [36] Mengyuan Jing, Yanmin Zhu, Tianzi Zang, and Ke Wang. 2023. Contrastive Self-supervised Learning in Recommender Systems: A Survey. *arXiv preprint arXiv:2303.09902* (2023).
- [37] Prannay Khosla, Piotr Teterwak, Chen Wang, Aaron Sarna, Yonglong Tian, Phillip Isola, Aaron Maschiot, Ce Liu, and Dilip Krishnan. 2020. Supervised contrastive learning. *NeurIPS* 33 (2020), 18661–18673.
- [38] Shigeru Kondo and Takashi Miura. 2010. Reaction-diffusion model as a framework for understanding biological pattern formation. *science* 329, 5999 (2010), 1616–1620.
- [39] Taeyoung Kong, Taeri Kim, Jinsung Jeon, Jeongwhan Choi, Yeon-Chang Lee, Noseong Park, and Sang-Wook Kim. 2022. Linear, or Non-Linear, That is the Question!. In *WSDM*. 517–525.
- [40] Yeon-Chang Lee, Sang-Wook Kim, and Dongwon Lee. 2018. gOCF: Graph-theoretic one-class collaborative filtering based on uninteresting items. In *AAAI*, Vol. 32.
- [41] Boyu Li, Ting Guo, Xingquan Zhu, Qian Li, Yang Wang, and Fang Chen. 2023. SGCL: siamese graph contrastive consensus learning for personalized recommendation. In *WSDM*. 589–597.
- [42] Yongkun Li and Yang Kuang. 2001. Periodic solutions of periodic delay Lotka-Volterra equations and systems. *J. Math. Anal. Appl.* 255, 1 (2001), 260–280.
- [43] Fan Liu, Zhiyong Cheng, Lei Zhu, Zan Gao, and Liqiang Nie. 2021. Interest-Aware Message-Passing GCN for Recommendation. In *TheWebConf (former WWW)*. 1296–1305.
- [44] Xiao Liu, Fanjin Zhang, Zhenyu Hou, Li Mian, Zhaoyu Wang, Jing Zhang, and Jie Tang. 2021. Self-supervised learning: Generative or contrastive. *IEEE Transactions on Knowledge and Data Engineering* 35, 1 (2021), 857–876.
- [45] Alfred J Lotka. 2002. Contribution to the theory of periodic reactions. *The Journal of Physical Chemistry* 14, 3 (2002), 271–274.
- [46] Kelong Mao, Jieming Zhu, Jinpeng Wang, Quanyu Dai, Zhenhua Dong, Xi Xiao, and Xiuqiang He. 2021. SimpleX: A Simple and Strong Baseline for Collaborative Filtering. In *CIKM*. 1243–1252.
- [47] Kelong Mao, Jieming Zhu, Xi Xiao, Biao Lu, Zhaowei Wang, and Xiuqiang He. 2021. UltraGCN: Ultra Simplification of Graph Convolutional Networks for Recommendation. In *CIKM*.
- [48] Atsushi Nomura, Makoto Ichikawa, Rismon Hasiholan Sianipar, and Hidetoshi Miike. 2008. Edge detection with reaction-diffusion equations having a local average threshold. *Pattern Recognition and Image Analysis* 18 (2008), 289–299.
- [49] Hoang Nt and Takanori Maehara. 2019. Revisiting graph neural networks: All we have is low-pass filters. *arXiv preprint arXiv:1905.09550* (2019).
- [50] Kenta Oono and Taiji Suzuki. 2020. Graph neural networks exponentially lose expressive power for node classification. In *ICLR*.
- [51] Aaron van den Oord, Yazhe Li, and Oriol Vinyals. 2018. Representation learning with contrastive predictive coding. *arXiv preprint arXiv:1807.03748* (2018).
- [52] Shaowen Peng, Kazunari Sugiyama, and Tsunenori Mine. 2022. Less is More: Reweighting Important Spectral Graph Features for Recommendation. In *SIGIR*. 1273–1282.

- [53] Zehra Pinar. 2021. An Analytical Studies of the Reaction-Diffusion Systems of Chemical Reactions. *International Journal of Applied and Computational Mathematics* 7, 3 (2021), 81.
- [54] Gerlind Plonka and Jianwei Ma. 2008. Nonlinear regularized reaction-diffusion filters for denoising of images with textures. *IEEE Transactions on Image Processing* 17, 8 (2008), 1283–1294.
- [55] Jiezhong Qiu, Qibin Chen, Yuxiao Dong, Jing Zhang, Hongxia Yang, Ming Ding, Kuansan Wang, and Jie Tang. 2020. GCC: Graph contrastive coding for graph neural network pre-training. In *KDD*. 1150–1160.
- [56] Alec Radford, Jong Wook Kim, Chris Hallacy, Aditya Ramesh, Gabriel Goh, Sandhini Agarwal, Girish Sastry, Amanda Askell, Pamela Mishkin, Jack Clark, et al. 2021. Learning transferable visual models from natural language supervision. In *ICML*. PMLR, 8748–8763.
- [57] T. Konstantin Rusch, Michael M. Bronstein, and Siddhartha Mishra. 2023. A Survey on Oversmoothing in Graph Neural Networks. *arXiv preprint arXiv:2303.10993* (2023).
- [58] Uwe Schmidt and Stefan Roth. 2014. Shrinkage fields for effective image restoration. In *CVPR*. 2774–2781.
- [59] Yifei Shen, Yongji Wu, Yao Zhang, Caihua Shan, Jun Zhang, B. Khaled Letaief, and Dongsheng Li. 2021. How Powerful is Graph Convolution for Recommendation?. In *CIKM*.
- [60] Yehjin Shin, Jeongwhan Choi, Hyowon Wi, and Noseong Park. 2023. An Attentive Inductive Bias for Sequential Recommendation Beyond the Self-Attention. *arXiv preprint arXiv:2312.10325* (2023).
- [61] Alan Turing. 1952. The chemical basis of morphogenesis. *Phil. Trans. R. Soc. Lond. B* (1952).
- [62] Greg Turk. 1991. Generating textures on arbitrary surfaces using reaction-diffusion. *Acm Siggraph Computer Graphics* 25, 4 (1991), 289–298.
- [63] Greg Turk. 1992. *Texturing surfaces using reaction-diffusion*. The University of North Carolina at Chapel Hill.
- [64] Xiang Wang, Xiangnan He, Meng Wang, Fuli Feng, and Tat-Seng Chua. 2019. Neural Graph Collaborative Filtering. In *SIGIR*.
- [65] Yifei Wang, Yisen Wang, Jiansheng Yang, and Zhouchen Lin. 2021. Dissecting the Diffusion Process in Linear Graph Convolutional Networks. In *NeurIPS*.
- [66] Yuelin Wang, Kai Yi, Xinliang Liu, Yu Guang Wang, and Shi Jin. 2023. ACMP: Allen-Cahn Message Passing for Graph Neural Networks with Particle Phase Transition. In *ICLR*.
- [67] Andrew Werth. 2015. Turing patterns in Photoshop. In *Proceedings of Bridges 2015: Mathematics, Music, Art, Architecture, Culture*. 459–462.
- [68] Andrew Witkin and Michael Kass. 1991. Reaction-diffusion textures. In *Proceedings of the 18th annual conference on computer graphics and interactive techniques*. 299–308.
- [69] Jiancan Wu, Xiang Wang, Fuli Feng, Xiangnan He, Liang Chen, Jianxun Lian, and Xing Xie. 2021. Self-Supervised Graph Learning for Recommendation. In *SIGIR*. 726–735.
- [70] Jun Xia, Lirong Wu, Juntao Chen, Bozhen Hu, and Stan Z. Li. 2022. SimGRACE: A Simple Framework for Graph Contrastive Learning without Data Augmentation. In *TheWebConf (former WWW)*.
- [71] Lianghao Xia, Chao Huang, Yong Xu, Jiashu Zhao, Dawei Yin, and Jimmy Huang. 2022. Hypergraph contrastive collaborative filtering. In *SIGIR*. 70–79.
- [72] Lianghao Xia, Chao Huang, and Chuxu Zhang. 2022. Self-supervised hypergraph transformer for recommender systems. In *KDD*. 2100–2109.
- [73] YuHao Xu, ZhenHai Wang, ZhiRu Wang, YunLong Guo, Rong Fan, HongYu Tian, and Xing Wang. 2023. SimDCL: dropout-based simple graph contrastive learning for recommendation. *Complex & Intelligent Systems* (2023), 1–13.
- [74] Yuning You, Tianlong Chen, Yongduo Sui, Ting Chen, Zhangyang Wang, and Yang Shen. 2020. Graph contrastive learning with augmentations. *NeurIPS* 33 (2020), 5812–5823.
- [75] Junliang Yu, Min Gao, Jundong Li, Hongzhi Yin, and Huan Liu. 2018. Adaptive implicit friends identification over heterogeneous network for social recommendation. In *CIKM*. 357–366.
- [76] Junliang Yu, Xin Xia, Tong Chen, Li zhen Cui, Nguyen Quoc Viet Hung, and H. Yin. 2022. XSimGCL: Towards Extremely Simple Graph Contrastive Learning for Recommendation. *arXiv preprint arXiv:2209.02544* (2022).
- [77] Junliang Yu, Hongzhi Yin, Xin Xia, Tong Chen, Lizhen Cui, and Quoc Viet Hung Nguyen. 2022. Are graph augmentations necessary? simple graph contrastive learning for recommendation. In *SIGIR*. 1294–1303.
- [78] Tao Zhou, Zoltán Kuscik, Jian-Guo Liu, Matúš Medo, Joseph Rushton Wakeling, and Yi-Cheng Zhang. 2010. Solving the apparent diversity-accuracy dilemma of recommender systems. *Proceedings of the National Academy of Sciences* 107, 10 (2010), 4511–4515.
- [79] Yanqiao Zhu, Yichen Xu, Feng Yu, Qiang Liu, Shu Wu, and Liang Wang. 2020. Deep graph contrastive representation learning. *arXiv preprint arXiv:2006.04131* (2020).
- [80] Yanqiao Zhu, Yichen Xu, Feng Yu, Qiang Liu, Shu Wu, and Liang Wang. 2021. Graph contrastive learning with adaptive augmentation. In *TheWebConf (former WWW)*. 2069–2080.